JOURNAL OF BACTERIOLOGY, Dec. 2001, p. 7231–7240 Vol. 183, No. 24
0021-9193/01/$04.00+0 DOI: 10.1128/JB.183.24.7231–7240.2001

Different Physiological Roles of ATP- and PP_i-Dependent Phosphofructokinase Isoenzymes in the Methylotrophic Actinomycete *Amycolatopsis methanolica*

A. M. C. R. ALVES,[1] G. J. W. EUVERINK,[1] H. SANTOS,[2] AND L. DIJKHUIZEN[1]*

Department of Microbiology, Groningen Biomolecular Sciences and Biotechnology Institute (GBB), University of Groningen, 9751 NN Haren, The Netherlands,[1] and Instituto de Tecnologia Quimica e Biologica, Universidade Nova de Lisboa, Apartado 127 Oeiras, Portugal[2]

Received 16 April 2001/Accepted 18 September 2001

Cells of the actinomycete *Amycolatopsis methanolica* grown on glucose possess only a single, exclusively PP_i-dependent phosphofructokinase (PP_i-PFK) (A. M. C. R. Alves, G. J. W. Euverink, H. J. Hektor, J. van der Vlag, W. Vrijbloed, D.H.A. Hondmann, J. Visser, and L. Dijkhuizen, J. Bacteriol. 176:6827–6835, 1994). When this methylotrophic bacterium is grown on one-carbon (C_1) compounds (e.g., methanol), an ATP-dependent phosphofructokinase (ATP-PFK) activity is specifically induced, completely replacing the PP_i-PFK. The two *A. methanolica* PFK isoenzymes have very distinct functions, namely, in the metabolism of C_6 and C_1 carbon substrates. This is the first report providing biochemical evidence for the presence and physiological roles of PP_i-PFK and ATP-PFK isoenzymes in a bacterium. The novel ATP-PFK enzyme was purified to homogeneity and characterized in detail at the biochemical and molecular levels. The *A. methanolica* ATP-PFK and PP_i-PFK proteins possess a low level of amino acid sequence similarity (24%), clearly showing that the two proteins are not the result of a gene duplication event. PP_i-PFK is closely related to other (putative) actinomycete PFK enzymes. Surprisingly, the *A. methanolica* ATP-PFK is most similar to ATP-PFK from the protozoon *Trypanosoma brucei* and PP_i-PFK proteins from the bacteria *Borrelia burgdorferi* and *Treponema pallidum*, both spirochetes, very distinct from actinomycetes. The data thus suggest that *A. methanolica* obtained the ATP-PFK-encoding gene via a lateral gene transfer event.

In many organisms, the phosphorylation of fructose-6-phosphate (F-6-P) to fructose-1,6-bisphosphate (F-1,6-P_2) is catalyzed by an ATP-dependent phosphofructokinase enzyme (ATP-PFK; EC 2.7.1.11) (30, 37). This irreversible ATP-PFK reaction is generally allosterically regulated and is considered to be a major point of regulation in glycolysis (18, 19, 21). However, a second type of PFK enzyme, using pyrophosphate (PP_i) as a substrate (but not ATP) (PP_i-PFK; EC 2.7.1.90) and catalyzing the reversible phosphorylation of F-6-P to F-1,6-P_2, exists in plants and in some bacteria and archaea (31). In bacteria, the PP_i-PFK is normally not regulated at the activity level. A third type of PFK enzyme, using ADP as a substrate (ADP-PFK; no EC number available), has been found in the extremophilic archaeon *Pyrococcus furiosus* and in other hyperthermophilic archaea, e.g., *Thermococcus* (24, 33).

In *Escherichia coli*, two ATP-PFK isoenzymes with different kinetic properties and no apparent sequence similarities have been identified (9, 25, 26). PFK1, which accounts for 90% of the total PFK activity (25), is an allosteric enzyme which displays cooperativity with respect to F-6-P and is regulated at the activity level by phosphoenolpyruvate (PEP; an inhibitor) and ADP and GDP (activators). The remaining 10% of PFK activity is accounted for by PFK2. The latter enzyme is not sensitive to PEP and only slightly inhibited by ATP and F-1,6-P_2. ADP affects PFK2 activity, with up to 50% inhibition at low F-6-P and ATP concentrations (17). It is unclear whether these two *E. coli* PFKs have distinct physiological roles (11).

Actinomycetes are best known for their ability to produce secondary metabolites (e.g., antibiotics). *Streptomyces* and *Amycolatopsis* species are especially widely used in industrial production processes. Antibiotics are derived from intermediates of primary metabolism, the availability of which may limit overall process productivity. Attempts to construct better-producing strains, therefore, also focus on elimination of possible bottlenecks in central metabolic pathways (e.g., glycolysis) (1) involved in glucose utilization. However, limited information is available about primary metabolism in actinomycetes. Previously, we characterized an ATP-PFK enzyme purified from glucose-grown cells of *Streptomyces coelicolor* A3(2) (2); this enzyme is allosterically inhibited by PEP. Studies with glucose-grown cells of the actinomycete *Amycolatopsis methanolica* revealed only a nonallosteric PP_i-PFK activity. This enzyme has been purified to homogeneity (a tetramer of 43,000-Da subunit size), and the corresponding gene (*pfp*) has been characterized (3, 4). PFK activity is also essential for the functioning of the ribulose monophosphate (RuMP) cycle of formaldehyde assimilation (fructose 1,6-bisphosphate [FBP] aldolase cleavage variant; Fig. 1) employed by *A. methanolica* during growth on one-carbon (C_1) compounds, e.g., methanol (13, 15, 16). However, no or only low PP_i-PFK activity levels could be detected in cells grown on C_1 compounds (references 3 and 13 and this study). Here, we report the biochemical and molecular characterization of a novel ATP-PFK enzyme that is specifically induced during growth of *A. methanolica* on C_1 compounds.

* Corresponding author. Mailing address: Department of Microbiology, University of Groningen, P.O. Box 14, 9750 AA Haren, The Netherlands. Phone: 31.50.3632150. Fax: 31.50.3632154. E-mail: L.Dijkhuizen@biol.rug.nl.

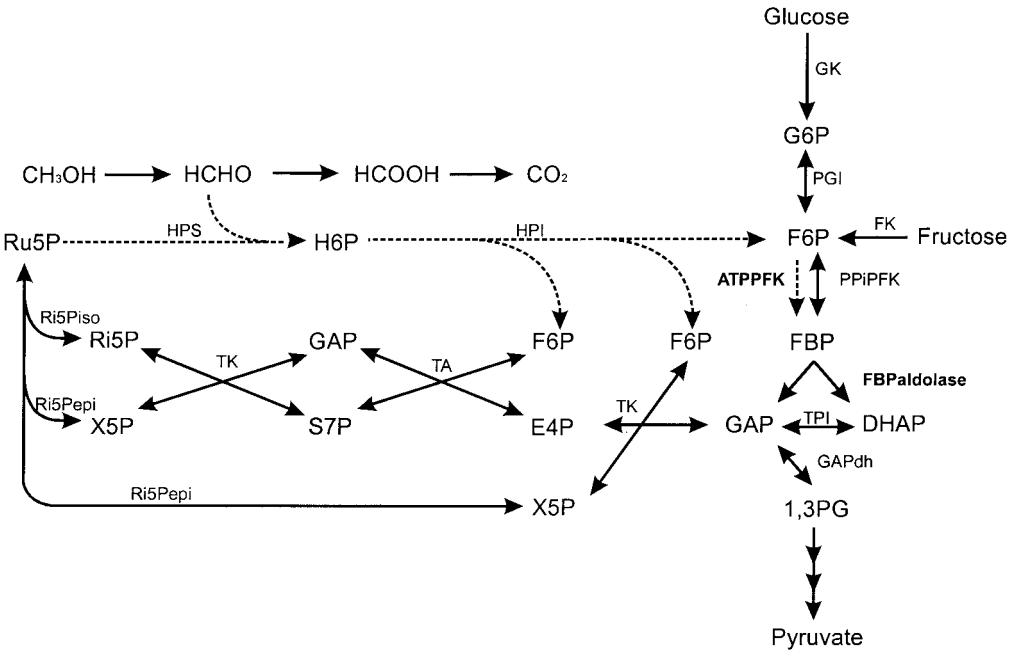

FIG. 1. Schematic representation of the pathways for glucose and methanol metabolism in *A. methanolica*. GK, glucose kinase; FK, fructose kinase; PGI, phosphoglucose isomerase; TA, transaldolase; TK, transketolase; $Ri5P_{epi}$, ribulose-5-phosphate epimerase; $Ri5P_{iso}$, ribulose-5-phosphate isomerase; TPI, triose phosphate isomerase, GAPdh, glyceraldehyde-3-phosphate dehydrogenase; S7P, sedoheptulose-7-phosphate; E4P, erythrose-4-phosphate; X5P, xylulose-5-phosphate; Ru5P, ribulose-5-phosphate; H6P, hexulose-6-phosphate; 1,3PG, 1,3-diphosphoglycerate; HPS, hexulose phosphate synthase; HPI, hexulose phosphate isomerase. The RuMP cycle enzymes specifically involved in the FBP aldolase cleavage variant (ATP-PFK and FBP aldolase) are shown by dashed lines.

MATERIALS AND METHODS

Bacterial strains, plasmids, and growth conditions. The plasmids and bacterial strains used are listed in Table 1.The plasmid pMEA300-free *A. methanolica* WVI strain (42) was grown at 37°C in batch cultures as described previously (13, 14). The medium was supplemented with various carbon sources at different concentrations (see Results). Sugars and organic acids were heat sterilized; amino acids, methanol, and formaldehyde were filter sterilized. Carbon-limited chemostats (working volume, 1 liter) were run at 37°C and pH 7.0 (controlled by automatic adjustment with 2 M NaOH). The medium contained (per liter) KH_2PO_4, 1.0 g; $(NH_4)_2SO_4$, 1.5 g; $MgCl_2$, 0.2 g; and 0.2 ml of a trace element solution (39). Formaldehyde-limited continuous cultures were established as described previously (20). The various measurements were performed on samples from cultures in transient state or steady state. A steady-state situation normally became established after five volume displacements.

Preparation of extracts, enzyme assays, and measurement of metabolite concentrations. Cells were washed in 50 mM Tris-HCl (pH 7.5) buffer containing 5 mM $MgCl_2$ and 5 mM dithiothreitol (buffer A). The cells were disrupted by three passages through a French pressure cell at 140 MPa, followed by centrifugation of the lysate at 40,000 × *g* for 30 min. The supernatant was used for all enzyme assays (at 37°C) and for purification of the ATP-PFK protein. Triton X-100 (0.01% [wt/vol]) was added to all reaction mixtures containing NADH in order to reduce endogenous NADH consumption. All enzyme assays were done in triplicate; the data presented are averages with a standard deviation of less than 10%. One unit is the amount of enzyme catalyzing the synthesis or the degradation of 1 μmol of product or substrate per min. PFK was assayed in a reaction mixture with 50 mM Tris-HCl buffer (pH 7.5), 5 mM $MgCl_2$, 1 mM KCl, 3 mM NH_4Cl, 5 mM dithiothreitol, 0.15 mM NADH, 10 mM F-6-P, 0.9 U of FBP aldolase, 5 U of triose phosphate isomerase, 0.85 U of α-glycerol-3-phosphate dehydrogenase, and limiting amounts of extract. The reaction was started by addition of 5 mM of PP_i (for PP_i-PFK) or 5 mM ATP (for ATP-PFK). PP_i and ATP solutions were adjusted to pH 7.5.

Preparation of cell extracts for NMR analysis. *A. methanolica* cells were grown on mineral medium with glucose or methanol and harvested at the end of the exponential growth phase. Cell extracts were prepared by injecting culture samples into liquid nitrogen (using a syringe) followed by addition of perchloric acid to a final concentration of 10% (vol/vol) and vigorously mixing the ingredients on ice for 20 min. The mixture was centrifuged at 20,000 × *g* for 10 min, and the supernatant was adjusted to neutral pH with 5 M potassium hydroxide. The preparation obtained was freeze-dried for further use. The residue was dissolved in water; EDTA was added to a final concentration of 10 mM, and the pH was adjusted to 8.2. ^{31}P nuclear magnetic resonance (NMR) spectra were acquired at 202.46 MHz with proton broadband decoupling in a Bruker AMX500 spectrometer and a 10-mm-long quadruple-nucleus probe head (^{31}P, ^{13}C, ^{15}N, and ^{1}H). The following acquisition parameters were typically used: spectral width, 12 kHz; pulse width, 18 μs (corresponding to a 70° flip angle); data size, 16 K; repetition delay, 3.8 s. For quantification of phosphorylated metabolites, the signal intensities in fully relaxed spectra (repetition delay, 30.8 s) were compared with the intensity of the resonance due to a known amount of sodium pyrophosphate

TABLE 1. Bacterial strains and plasmids used in this study

Strain or plasmid	Relevant genotype	Source or reference
A. methanolica WVI	pMEA300-free derivative strain of *A. methanolica* NCBI 11946	42
E. coli DH5α	*supE44 ΔlacU169* (ϕ80*lacZΔM15*)*hsdR17 recA1 endA1 gyrA96 thi-1 relA1*	Bethesda Research Laboratories
Plasmids		
PDA71	*Rhodococcus-E. coli* shuttle vector; *cat ecoRI bla*	10
pBluescript KS(+)	Amp^r; phagemid derived from pUC18; *lacZ*	Stratagene
PAM101	5-kb *Bam*HI DNA fragment containing *pfk* ligated in *Bgl*II-digested pDA71	This study

added to the sample. Identification of resonances was made by adding small amounts of suspected compounds to the sample and observing the increase in the intensity of resonances in the spectrum. The presence of ADP, UDP, ATP, UTP, UMP, UDP-*N*-acetylglucosamine, and PP_i was detected in this way. Polyphosphate was identified from the characteristic chemical shift at approximately −22 ppm. Chemical shifts are referenced with respect to external 85% H_3PO_4.

Purification of ATP-PFK enzyme. All chromatographic steps were carried out in a System Prep 10 liquid chromatography system (Pharmacia LKB Biotechnology Inc.) at room temperature. Collected fractions were immediately placed on ice.

(i) Step 1. Methanol (100 mM)-grown cells were harvested from a batch culture of *A. methanolica* WVI at the end of the exponential growth phase. Extracts were prepared in buffer A as described before.

(ii) Step 2. Ammonium sulfate precipitation. Solid $(NH_4)_2SO_4$ was slowly added to the preparation from step 1 to 30% saturation and stirred for 20 min. The mixture was then centrifuged at 40,000 × *g* for 15 min. The pellet was resuspended in a minimum volume of buffer A and dialyzed overnight against the same buffer.

(iii) Step 3. Affinity chromatography. A sample from step 2 was applied to a Levafix Blue G-3A-Sepharose CL-4B (24) column (30 ml) previously equilibrated with buffer A. The column was washed with 3 volumes of buffer A, and ATP-PFK was eluted with buffer A containing 300 mM $(NH_4)_2SO_4$ (flow rate, 3 ml · min^{-1}; fractions, 4 ml).

(iv) Step 4. Anion-exchange chromatography. Protein from step 3 was applied to a Resource Q column previously equilibrated with buffer A (flow rate, 2 ml · min^{-1}). Bound proteins were eluted with a linear gradient of 0 to 0.4 M NaCl in buffer A. Fractions containing ATP-PFK activity were pooled, and solid $(NH_4)_2SO_4$ was slowly added until 30% saturation.

(v) Step 5. Hydrophobic interaction chromatography. Protein from step 4 was applied to a Phenyl-Superose column (HR5/5) previously equilibrated with buffer A plus 30% $(NH_4)_2SO_4$ (flow rate, 0.5 ml · min^{-1}). Bound proteins were eluted with a linear decreasing gradient from 30 to 0% $(NH_4)_2SO_4$ in buffer A. Fractions containing ATP-PFK activity were pooled, and glycerol was added to a final concentration of 40% (vol/vol) before storage at −20°C.

Estimation of molecular mass. The relative molecular mass of the active enzyme was estimated by gel filtration in buffer A on a Superdex 200 column (XK 16/60) at a flow rate of 1 ml · min^{-1} with thyroglobulin (molecular mass, 670,000 Da), gamma globulin (158,000 Da), ovalbumin (44,000 Da), myoglobin (17,000 Da), and cobalamine (1,350 Da) as gel filtration standards.

Estimation of subunit size. Sodium dodecyl sulfate (SDS)-polyacrylamide gel electrophoresis (27) was performed with the following prestained marker proteins: phosphorylase B (106,000 Da), bovine serum albumin (80,000 Da), ovalbumin (49,500 Da), carbonic anhydrase (32,500 Da), soybean trypsin inhibitor (27,500 Da), and lysozyme (18,500 Da) (Bio-Rad). The gels were stained by the silver-staining method (43).

Protein determination. Protein concentrations were determined with the Bio-Rad protein determination kit with bovine serum albumin as a standard (8).

Kinetic studies. Kinetic parameters were determined at 37°C and pH 7.5 and were calculated with Sigma Plot for Windows 2000 (Jandell Scientific Software) using curve fitting with the Hill or Michaelis-Menten equation. Possible effectors (pH adjusted; at 1 and 4 mM final concentrations) of ATP-PFK were added separately to assays with purified enzyme, at near-K_m or K_{50} (concentration of the substrate at half V_{max} in non-Michaelis-Menten kinetics) concentrations of the substrates F-6-P and ATP in the presence of 5 mM $MgCl_2$.

Automated amino acid analysis. For determination of the N-terminal amino acid sequence, about 100 pmol of purified protein was applied to a Pro-spin cartridge (Applied Biosystems, Warrington, United Kingdom) containing a polyvinylidene difluoride membrane according to the manufacturer's protocol. Automated sequencing was performed at Eurosequence BV (Groningen, The Netherlands) on an automatic pulse liquid sequenator (model 477 A; Applied Biosystems) equipped on-line with a reverse-phase high-performance liquid chromatography unit (model 120 A; Applied Biosystems).

Peptide digest and amino acid sequence. The purified ATP-PFK was digested with trypsin. The resultant peptides were separated by reverse-phase high-performance liquid chromatography using a Nucleosil 10C18 column equilibrated with 0.1% trifluoroacetic acid and eluted with a gradient of 0 to 100% 0.1% trifluoroacetic acid plus 100% acetonitrile over 120 min at a flow rate of 1 ml · min^{-1}. The amino acid sequence of the peptide eluting in fraction 45 (at 48 min) was analyzed as described above.

DNA manipulations. Chromosomal DNA (40) and plasmid DNA (7) were isolated as described previously. DNA-modifying enzymes were obtained from Boehringer (Mannheim, Germany) and were used according to the manufacturer's instructions.

TABLE 2. Enzyme activities in *A. methanolica* WVI cells grown in batch culture on different substrates

Substrate	Specific activity (mU · mg^{-1})	
	PP_i-PFK	ATP-PFK
Glucose (10 mM)	180	0
Fructose (10 mM)	120	0
Glycerol (20 mM)	100	0
Acetate (20 mM)	20	0
Gluconate (10 mM)	30	0
Succinate (10 mM)	20	0
Phenylalanine (10 mM)	30	0
Methanol (60 mM)	20	120
Formaldehyde[a] (50 mM)	10	220
Betaine (20 mM)	10	180

[a] Data from formaldehyde-limited continuous cultures in steady-state at a growth rate of *D* (dilution rate) = 0.05 h^{-1}.

Southern hybridizations. Chromosomal DNA from *A. methanolica*, digested with the appropriate enzymes, was subjected to electrophoresis on a 0.8% agarose gel and transferred to a nylon-Plus membrane (Qiagen, Basel, Switzerland) after alkaline denaturation (32). The membrane was probed at 62°C with an oligonucleotide probe (100 pmol) labeled with the DIG oligonucleotide tailing kit from Boehringer. The membrane was subsequently washed twice with 2× SSC (1× SSC is 0.15 M NaCl plus 0.015 M sodium citrate)–0.1% [wt/vol] SDS for 5 min and twice with 0.1× SSC–0.1% SDS for 5 min.

Construction of a partial genomic library and cloning of the *pfk* gene. Chromosomal DNA from *A. methanolica* was digested overnight with the restriction enzyme *Bam*HI and subjected to sucrose fractionation. DNA fragments varying in size (0.5 to 20 kb) were collected by centrifugation (Sorvall SW-28 rotor) for 24 h at 122,000 × *g*. Each fraction (500 μl) was dialyzed overnight against water to remove the sucrose. Subsequently, 5 μl of each fraction was subjected to electrophoresis and transferred to a nylon-Plus membrane. Southern hybridizations were performed at 62°C with 2 digoxigenin-labeled degenerated oligonucleotide probes (oligo 1, GAA/G CCG/C GCG/C GAG/A TTC GGC/G GCG/C GTG/C GCG/C GCG/C CGC/G, derived from the peptide QPAEFGAVAAR; and oligo 2, AAC GAA/G GTG/C GAC CCG/C GAC GGG/C GAC CTG/C TGG ATG, derived from the peptide NQVDPDGDLWM), both corresponding to the internal peptide sequence obtained by trypsin digestion of the purified ATP-PFK protein. Both oligonucleotides hybridized with the same 4.4-kb band, confirming that both probes specifically hybridized to the *pfk* gene. Subsequently, DNA fragments ranging from 4 to 5 kb in size were ligated into the *Bgl*II site of plasmid pDA71 and transformed to *E. coli* DH5α. A positive clone (pAM101) was identified via hybridization and further characterized by restriction analysis and nucleotide sequencing.

Nucleotide sequencing. Double-stranded DNA was sequenced with T7 polymerase, with unlabeled primers and fluorescein-labeled ATP (41). The nucleotide sequence data was compiled and analyzed using the programs supplied in the PC/GENE software package (Intelligenetics, Mountain View, Calif.).

Sequence comparison and phylogenetic-tree construction. The PFK alignment was made with Clustal W (36); positions with fully conserved amino acid residues, positions with fully conserved strong groups (STA, NEQK, NHQK, NDEQ, QHRK, MILV, MILF, HY, and FYW), and positions with fully conserved weaker groups (CSA, ATV, SAG, STNK, STPA, SGND, SNDEQK, NDEQHK, NEQHRK, FVLIM, and HFY) are indicated by the program. The groups are according to the Pam 250 residue matrix. The programs supplied in Treecon (38) were used to determine phylogenetic relationships among the PFK proteins. Bootstrap values (100 replicates) were performed to evaluate the reliability of the tree.

Nucleotide sequence accession number. The nucleotide sequence presented in this paper was entered into GenBank under accession number AF298119.

RESULTS

PP_i-PFK and ATP-PFK activities in cells grown on different carbon substrates. As shown previously, only PP_i-PFK activity is present in *A. methanolica* cells grown on glucose (3, 4) (Table 2). We observed that cells grown on methanol possess a significant ATP-PFK activity. When we screened several

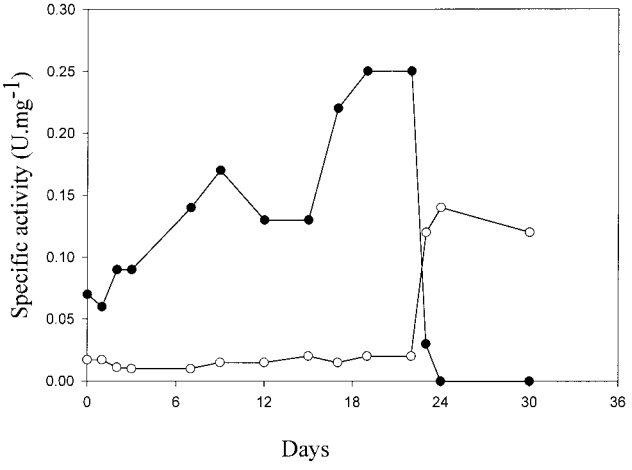

FIG. 2. Profiles of ATP- and PP_i-dependent PFK activities in cell extracts of *A. methanolica* grown in carbon- and energy source-limited continuous culture on the substrates glucose, formaldehyde, and methanol at a growth rate of *D* (dilution rate) = 0.05 h^{-1}. Days 0 to 6, 50 mM methanol; days 6 to 10, 50 mM methanol plus 5 mM formaldehyde; days 10 to 14, 50 mM methanol plus 12 mM formaldehyde; days 14 to 22, 50 mM formaldehyde; day 22 to end, 5 mM glucose. ●, ATP-PFK; ○, PP_i-PFK.

growth substrates, it appeared that ATP-PFK activity became specifically induced when the organism was grown on C_1 substrates or on betaine (Table 2). Degradation of betaine results in formaldehyde release that is assimilated via the RuMP cycle. Similar observations were made when *A. methanolica* was grown in carbon-limited chemostat cultures (Fig. 2). ATP-PFK activity was present in cells grown under methanol or formaldehyde limitation only. During growth on glucose, ATP-PFK activity completely disappeared and only PP_i-PFK activity was detected. A similar regulatory pattern of induction (by C_1 compounds) and repression (by glucose) was observed for the RuMP cycle enzymes hexulose-6-phosphate synthase (HPS) and hexulose-6-phosphate isomerase (HPI) involved in assimilation of C_1 compounds (references 3 and 13 and this study). The various observations indicate that PP_i-PFK and ATP-PFK have different physiological roles. ATP-PFK is specifically involved in the RuMP cycle of formaldehyde assimilation during growth on C_1 compounds; PP_i-PFK functions in the glycolytic pathway (Fig. 1).

Purification and characterization of ATP-PFK. The ATP-PFK enzyme was purified to homogeneity (1,230-fold, with a final yield of 23%) from methanol-grown cells. The ATP-PFK binds to a Levafix blue G-3A-Sepharose Cl-4B column (22), resulting in a 294-fold purification in a single step (Table 3). Subsequent anion-exchange (Resource Q) and hydrophobic-interaction (Phenyl-Superose) column chromatography yielded a homogeneous preparation of ATP-PFK, as judged by SDS-polyacrylamide gel electrophoresis and silver staining.

TABLE 3. Purification of ATP-PFK from methanol-grown cells of *A. methanolica* WVI

Step	Procedure	Protein (mg)	Total activity (U)	Sp act (U · mg^{-1})	Purification (fold)	Yield (%)
1	Crude extract	160	20.8	0.13	1	100
2	$(NH_4)_2SO_4$ (30%)	80	13.6	0.17	1.3	65
3	Levafix blue	0.2	10	50	385	48
4	Resource Q	0.08	7.2	90	692	35
5	Phenyl-Superose	0.03	4.8	160	1,230	23

Characterization of the pure ATP-PFK enzyme revealed an M_r of 110,000 for the holoenzyme and a subunit size of 50,000, suggesting a dimeric structure. The enzyme stored in buffer with 40% glycerol at −20°C retained its full activity over a period of 6 months.

The enzyme showed an absolute specificity for its substrate, F-6-P, which could not be replaced by fructose-1-phosphate or glucose-6-phosphate. The phosphate donor ATP could be replaced by GTP or UTP with a remaining activity of 100 and 40%, respectively. Also, Mg^{2+} ions were essential for ATP-PFK activity, with an apparent K_m for Mg^{2+} of about 0.025 mM (data not shown). Similar observations with respect to substrate specificity have been made for ATP-PFK enzymes from other bacterial sources (18).

Several metabolites (at 1 and 4 mM final concentrations) were tested for effects on ATP-PFK activity, with 5 mM F-6-P and Mg^{2+} and 1 mM ATP present. PP_i caused 20 and 50% inhibition, and AMP caused 20 and 40% inhibition (at 1 and 4 mM), respectively. ADP, citrate, PEP, FBP, sedoheptulose-7-P, erythrose-4-P, pyruvate, xylulose-5-P, ribulose-5-P, and sedoheptulose-7-phosphate (all at 1 and 4 mM concentrations except for fructose 2,6-bisphosphate at 0.1 mM) had no effect on ATP-PFK enzyme activity.

Kinetics of the ATP-PFK enzyme. The kinetic parameters of the purified ATP-PFK enzyme were determined in the presence of 5 mM Mg^{2+} (Fig. 3 and Table 4). Michaelis-Menten kinetics was observed with respect to ATP (Fig. 3A). The apparent K_m value for ATP was estimated as 0.6 ± 0.1 mM. PP_i was an inhibitor of ATP-PFK, decreasing the V_{max} and affinity of the enzyme for ATP. With 2 and 4 mM PP_i (Fig. 3A and Table 4), the data points could be better fitted with the Hill equation, giving a K_{50} value for ATP of 1.0 to 1.5 ± 0.1 mM with a Hill coefficient (*n*) of 2. With respect to the affinity of the enzyme for the substrate F-6-P, all data points could be better fitted with the Hill equation. PP_i also decreased the V_{max} and affinity of the enzyme for the substrate F-6-P. The affinity for F-6-P was rather low and varied between K_{50} values of 6 and 10 mM (Fig. 3B and Table 4) with a Hill coefficient of 2.

N-terminal amino acid sequence. The first 26 amino acids of the ATP-PFK protein were determined (in two separate experiments) to be TLHLDDLRVRLLGERRYDSPFXEVRHT. Surprisingly, no homology was observed with PFK enzyme sequences present in databases or with any other class of proteins. When we compared the initial yield for the automated protein sequencing (ca. 40 and 45 pmol) with the amount of protein applied to the membrane used (ca. 50 pmol), we concluded that the sequence obtained was from the purified ATP-PFK protein and not from a possible contaminant.

Internal peptide sequence. The amino acid sequence of one peptide in the ATP-PFK tryptic digest (NQVDPDGDLWMSV LETTXQPAEFGAVAAR) was further analyzed, resulting in identification of a further 28 amino acids. Database searches using this sequence as the query again revealed no similarity with known PFK proteins or with any other class of proteins.

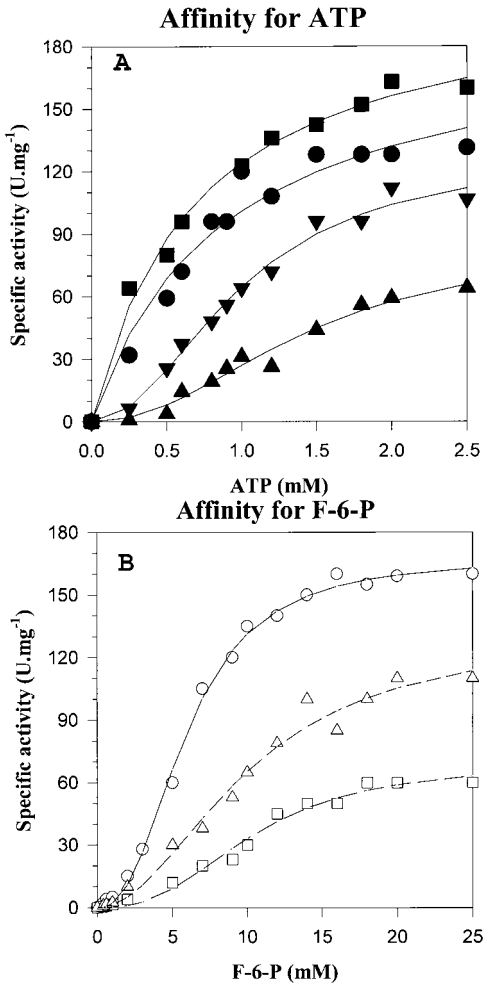

FIG. 3. Kinetics of ATP-PFK from *A. methanolica* and effect of PP_i on ATP-PFK activity. (A) ATP-PFK activity versus ATP concentration at a fixed F-6-P concentration (10 mM). ■, 0 mM PP_i; ●, 1 mM PP_i; ▼, 2 mM PP_i; ▲, 4 mM PP_i. (B) ATP-PFK activity versus F-6-P concentration at fixed ATP concentrations. ○, 0 mM PP_i; △, 2 mM PP_i; □, 4 mM PP_i. Kinetic parameters are given in Table 4.

Cloning, sequencing, and analysis of the *A. methanolica pfk* gene. The strategy used for isolation of the *pfk* gene from *A. methanolica* was to design two oligonucleotide probes (see Materials and Methods) based on the internal peptide amino acid sequence. Initial hybridizations on digested genomic DNA with both probes yielded a unique 4.4-kb hybridization signal. We therefore concluded that both probes specifically hybridized to the *pfk* gene. Screening of a partial genomic library (1,500 transformants) yielded pAM101. Nucleotide sequencing of the 5-kb pAM101 insert revealed an open reading frame (ORF) of 1,379 bp coding for a polypeptide of 459 amino acids with a calculated molecular mass of 48,500 Da. The G+C content of this ORF (70%) is similar to the high G+C content of other *A. methanolica* and *S. coelicolor* genes and of other actinomycete genomes (1, 2, 4, 44). A total of 23 out of the 26 amino acids identified in the ATP-PFK N-terminal amino acid sequence were found in the deduced amino acid sequence; the internal peptide sequence of 28 amino acids could be perfectly identified in this sequence. Database searches using the deduced amino acid sequence as the query revealed high similarity scores with other PFK proteins (see below). We conclude that this ORF encodes the *A. methanolica* ATP-PFK protein.

TABLE 4. Kinetics of the ATP-PFK enzyme from *A. methanolica* WVI and effects of PP_i on affinities for substrates F-6-P and ATP

Substrate	$V_{max_{app}}$ (U · mg^{-1})	K_{app} (mM)	K_{50} (mM)	*n*	PP_i (mM)
ATP[a]	180 ± 4.0	0.6 ± 0.1			Absent
	130 ± 5.0	0.9 ± 0.07			1
	110 ± 5.0		1.0 ± 0.1	2	2
	60 ± 4.0		1.5 ± 0.1	2	4
F-6-P[b]	167 ± 3.0		6.0 ± 0.17	2	Absent
	100 ± 1.2		10 ± 1.0	2	2
	80 ± 5		10 ± 0.8	2	4

[a] At [F-6-P] = 10 mM.
[b] At [ATP] = 1 mM.

Sequence comparison of PFK proteins. The *A. methanolica* PFK amino acid sequences were aligned with those of other ATP-PFK and PP_i-PFK proteins from various sources. A subset of the full alignment (available on request) is shown in Fig. 4. In particular, the comparison between the *A. methanolica* ATP-PFK and PP_i-PFK enzymes and the *S. coelicolor* A3(2) ATP-PFK enzyme yielded surprising and interesting results. Only 24% similarity was observed between the two *A. methanolica* PFK proteins, while 70% identity was observed between the *S. coelicolor* A3(2) ATP-PFK and the *A. methanolica* PP_i-PFK (2, 4). Similarity between the ATP-PFKs from *A. methanolica* and *S. coelicolor* A3(2) was also low (23%).

Based on the three-dimensional crystal structure of the *E. coli* ATP-PFK enzyme (34), a total of 11 amino acid residues involved in binding of the F-6-P substrate have been identified. Identical residues are present in *S. coelicolor* A3(2) ATP-PFK and in *A. methanolica* PP_i-PFK (Fig. 4); 7 of the 11 residues could be identified in *A. methanolica* ATP-PFK (Fig. 4). Interestingly, the same four residues varied in ATP-PFK from the protozoon *Trypanosoma brucei* and in PP_i-PFK from the bacterium *Treponema pallidum* (Fig. 4). The mutations Arg 162 Ser and Arg 243 Ser in the *E. coli* ATP-PFK drastically decreased the affinity of the enzyme for F-6-P (6), in line with the low affinity of the *A. methanolica* ATP-PFK for F-6-P.

With respect to the amino acid residues assigned for the binding of ATP in *E. coli* PFK, the situation in the *A. methanolica* ATP-PFK enzyme differs more drastically: 8 out of 10 residues assigned for ATP binding in the *E. coli* PFK enzyme are not conserved in the *A. methanolica* ATP-PFK enzyme (Fig. 4). As previously noted (2), not all the residues involved in ATP binding in *E. coli* ATP-PFK are conserved in the ATP-PFK of *S. coelicolor* A3(2). Remarkably, the same differences were observed in the PP_i-PFK of *A. methanolica*. We observed that the ATP-PFK and PP_i-PFK enzymes of *A. methanolica* are quite distinct with respect to the identities of these residues. In fact, in this respect the *A. methanolica* ATP-PFK more closely resembles the *T. brucei* ATP-PFK and the *T. pallidum* PP_i-PFK (Fig. 4).

Phylogenetic relationships with other PFKs. A phylogenetic tree of PFK enzymes, based on alignment of full-length protein sequences, clearly showed that the previously characterized *S. coelicolor* A3(2) ATP-PFK (PFK1) (2) and *A. methanolica*

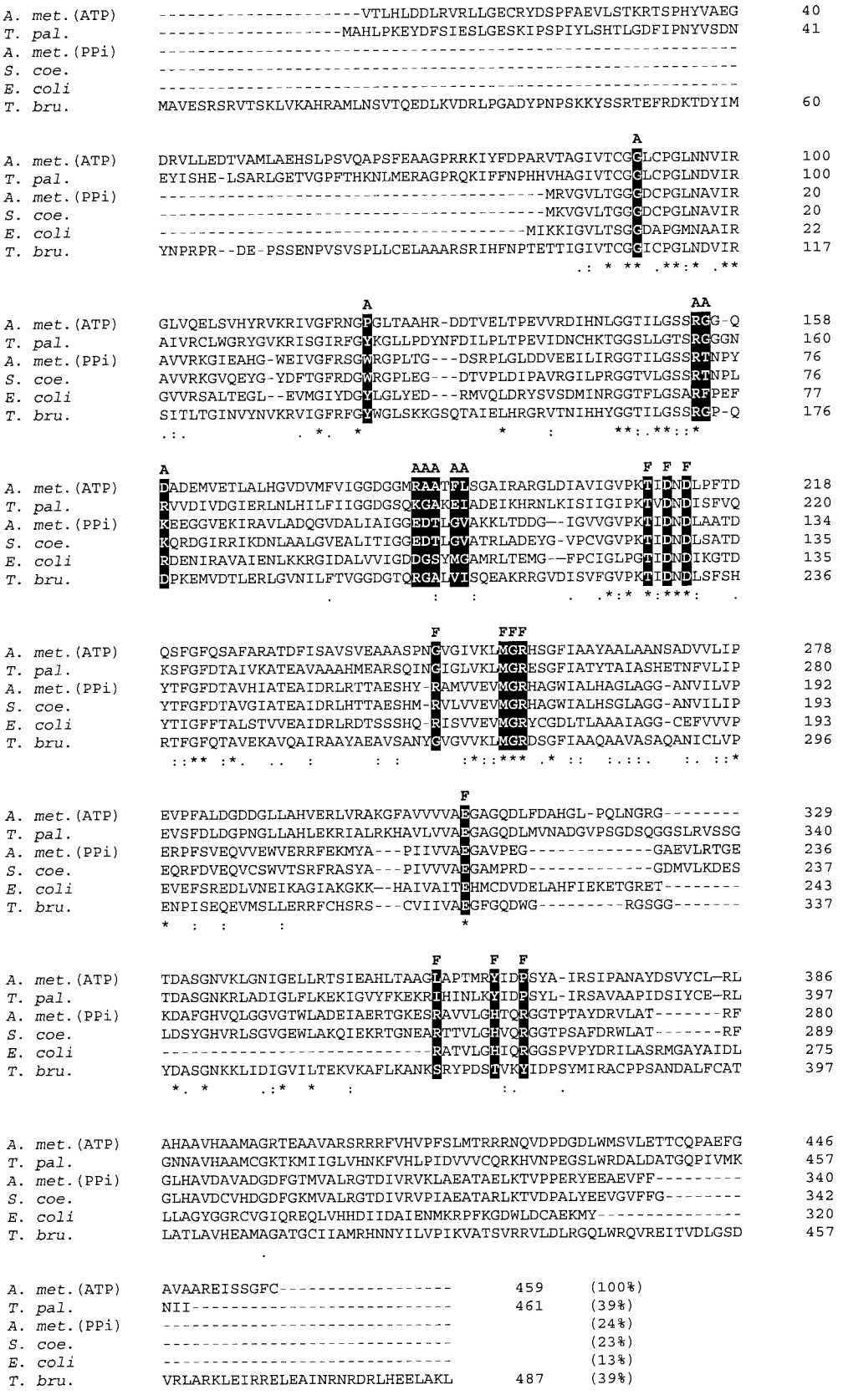

FIG. 4. Clustal W (36) multiple alignment of the deduced amino acid sequence of the ATP-PFK from *A. methanolica* with the sequences of the PFKs from *S. coelicolor* A3(2) (National Center for Biotechnology Information [NCBI] accession number 008333), *E. coli* (NCBI accession number KIECFA), *T. pallidum* (NCBI accession number A71366), and *T. brucei* (NCBI accession number AAC47836) and the PP_i-PFK from

PP_i-PFK (4) are closely related (Fig. 5). Additional putative actinomycete PFKs have been identified in the genome sequences of *Mycobacterium tuberculosis* (http://www.tigr.org/tdb), *Mycobacterium leprae* (http://www.sanger.ac.uk/projects/M-leprae), and *S. coelicolor* A3(2) (PFK2 and PFK3) (http://www.sanger.ac.uk/projects/S-coelicolor). Most actinomycete PFK proteins cluster closely together phylogenetically (Fig. 5). A clear exception is the novel ATP-PFK of *A. methanolica*, which shares little sequence similarity with the other six actinomycete PFKs. In fact, the ATP-PFK from *A. methanolica* is clearly more closely related to the ATP-PFK of the protozoon *T. brucei* and the PP_i-PFKs of the spirochetes *Borrelia burgdorferi* and *T. pallidum* (Fig. 5). These data thus suggest that *A. methanolica* has obtained the ATP-PFK enzyme via lateral gene transfer rather than via gene duplication events.

^{31}P-NMR analysis of *A. methanolica* cell extracts of glucose- and methanol-grown cultures. Aqueous suspensions of lyophilized *A. methanolica* cells grown on mineral medium with methanol (Fig. 6A) or glucose (Fig. 6B) as a carbon substrate were subjected to ^{31}P-NMR for identification of phosphocompounds. Striking differences were observed between the two growth conditions. (i) Interestingly, PP_i appeared only in glucose-grown cells (5 nmol · mg [dry weight]$^{-1}$). Much larger amounts of longer-chain inorganic polyphosphates were detected in methanol-grown cells. (ii) In methanol-grown cells, using the RuMP cycle (Fig. 1), a greater variety of phosphomonoesters, e.g., sugar phosphates (including F-6-P) and UMP, appeared. (iii) In glucose-grown cells, ADP, ATP, UDP, and UTP are present at similar levels ([ATP] = [UTP] = 2.4 nmol · mg [dry weight]$^{-1}$, [UDP] = 3.8 nmol · mg [dry weight]$^{-1}$, and [ADP] = 4.4 nmol · mg [dry weight]$^{-1}$). (iv) UDP was by far the major nucleotide in methanol-grown cells (4.5 nmol · mg [dry weight]$^{-1}$); other nucleotides were detected, but only in small amounts ([ADP] = 1 nmol · mg [dry weight]$^{-1}$ and [UDP-*N*-acetylglucosamine] = 2 nmol · mg [dry weight]$^{-1}$). The level of nucleotide triphosphates in these cells was also very low compared with that in glucose cells. (v) UDP-hexoses also accumulated at higher levels in methanol-grown cells. Two major UDP-hexose compounds were present. One of these was identified as UDP-*N*-acetylglucosamine. The other compound had resonances that did not coincide with UDP-glucose, UDP-glucuronic acid, or UDP-glucosamine, and it remained unidentified.

DISCUSSION

This is the first report providing biochemical evidence for the presence and physiological roles of ATP-PFK and PP_i-PFK isoenzymes in a bacterium, the actinomycete *A. methanolica*. ATP-PFK and PP_i-PFK isoenzymes had previously been reported only in higher plants (5). The two PFK isoenzymes differ in subunit composition and native molecular mass: the ATP-PFK is a dimer with 50-kDa subunits, whereas the PP_i-PFK is a tetramer with 43-kDa subunits.

The *A. methanolica* ATP-PFK and PP_i-PFK enzymes are clearly very different biochemically (see above), at the amino acid sequence level (24% similarity), phylogenetically (Fig. 5), with respect to the regulation of their synthesis (presence in cells grown on C_1 substrates and on sugars, respectively [Table 2]), and with respect to regulation of their activities (Table 4 and Fig. 3). On the basis of these observations, we conclude that earlier in the evolution of the *A. methanolica* genome the ATP-PFK-encoding gene was acquired via a lateral gene transfer phenomenon.

PFK activity in *A. methanolica* is required not only for sugar metabolism via the glycolytic pathway (serving both in energy generation and the synthesis of precursors for the synthesis of cell material) but also for the functioning of the RuMP cycle of formaldehyde assimilation (FBP aldolase cleavage variant; serving primarily in carbon assimilation) during growth on C_1 compounds (Fig. 1) (13, 15, 16). Similar to the typical RuMP cycle enzymes HPS and HPI, ATP-PFK (but not PP_i-PFK) is clearly induced by C_1 compounds and repressed by glucose. This ATP-PFK enzyme thus has a specific physiological role in the RuMP cycle during growth on C_1 compounds, whereas PP_i-PFK makes its most important contribution during growth on sugars (C_6 compounds) in the glycolytic pathway.

The *A. methanolica* ATP-PFK has a poor affinity for F-6-P (between 6 and 10 mM, depending on the ATP concentration). By comparison, the PP_i-PFK enzyme has a relatively high affinity for F-6-P (0.4 mM) (3). Most PFK enzymes have an affinity for F-6-P on the order of less than 1 mM (18). The ATP-PFK enzyme assayed in cell extracts displayed an affinity for F-6-P in the same order of magnitude (data not shown), ruling out the possible existence of an activator for this enzyme in vivo. PFK enzymes specifically functioning in the RuMP cycle have not been characterized before. This property of low F-6-P affinity thus may reflect the specific role of ATP-PFK in the RuMP cycle. Assimilation of three formaldehyde molecules via the RuMP cycle, with RuMP as an acceptor molecule, results in the net formation of three F-6-P molecules (Fig. 1). One molecule of F-6-P is converted via PFK and FBP aldolase, providing the cells two molecules of GAP/DHAP, the precursor for biosynthesis of cell material from pyruvate onwards. The two remaining F-6-P molecules, together with the second GAP/DHAP molecule, are used by transaldolase and transketolase enzymes in regeneration of three molecules of RuMP, involving a number of reversible enzyme steps. To ensure a sufficient regeneration of RuMP for formaldehyde assimilation, ATP-PFK action is required only when intracellular F-6-P levels have become rather high.

Glucose metabolism results in relatively high intracellular PP_i levels (Fig. 6), which may inhibit activity of the RuMP cycle ATP-PFK (Table 4). This, and the repression of the synthesis

A. methanolica (NCBI accession number Q59126). The percent similarity between the ATP-PFK from *A. methanolica* and each of the other PFKs is indicated in parentheses. A and F indicate residues (solid boxes) involved in binding of ATP and F-6-P, respectively, in the *E. coli* ATP-PFK enzyme (34). *, position with a fully conserved amino acid residue; :, position with a fully conserved strong group (STA, NEQK, NHQK, NDEQ, QHRK, MILV, MILF, HY, and FYW); ., position with a fully conserved weaker group (CSA, ATV, SAG, STNK, STPA, SGND, SNDEQK, NDEQHK, NEQHRK, FVLIM, and HFY).

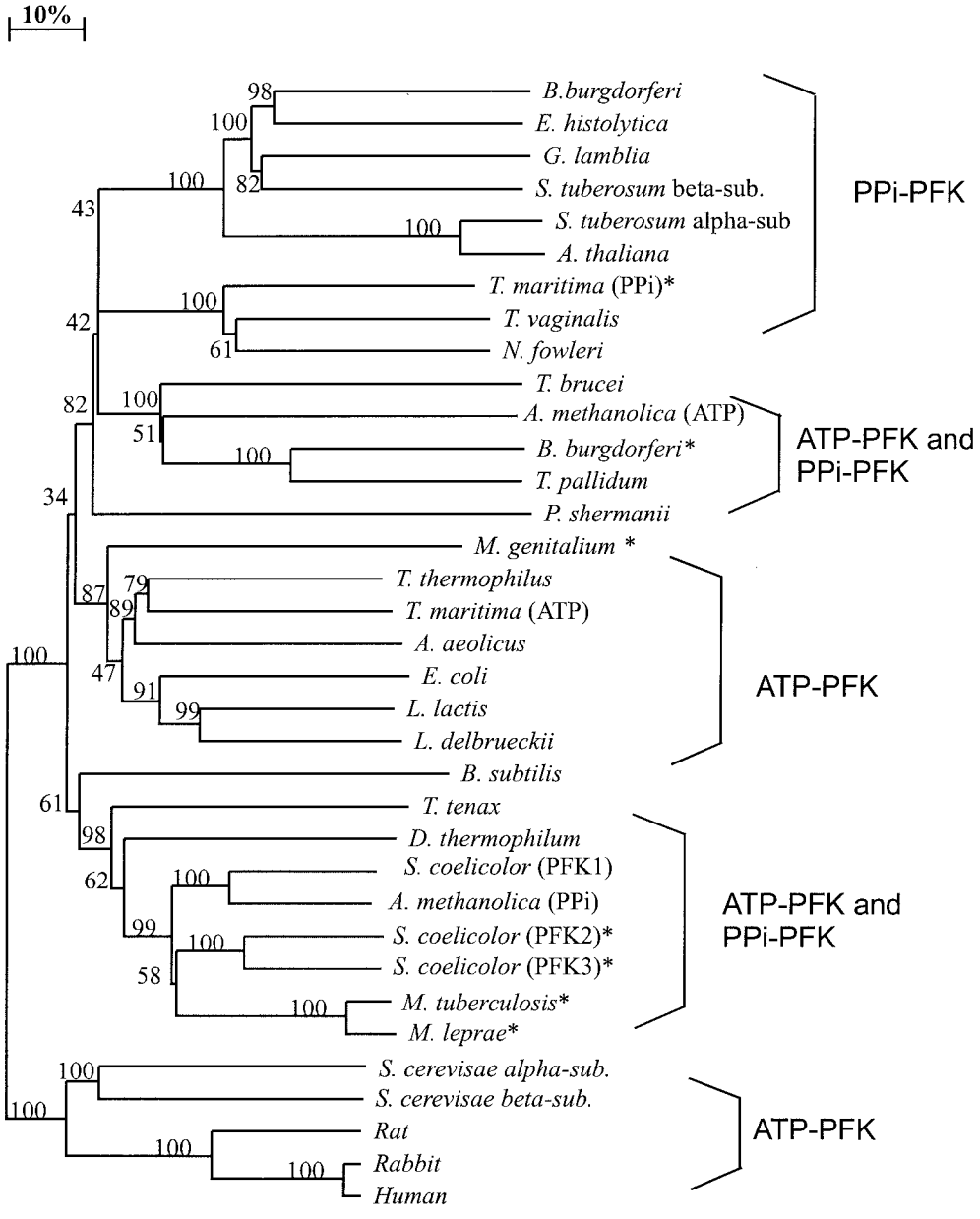

FIG. 5. Unrooted phylogenetic tree of PFK proteins. The tree is based on distance analysis (neighbor-joining method) of selected available sequences of ATP-PFK and PP_i-PFK proteins from the following sources in the National Center for Biotechnology Information database (accession numbers are given in parentheses): *B. burgdorferi* (D70102), *Entamoeba histolytica* (S68243), *Giardia lamblia* (S52081), *Solanum tuberosum* beta subunit (P21343), *S. tuberosum* alpha subunit (A36094), *Arabidopsis thaliana* (AC015450.3), *Thermotoga maritima* (PP_i-PFK) (G72396), *Trichomonas vaginalis* (AAD13344), *Naegleria fowleri* (S54978), *T. brucei* (AAC47836), *A. methanolica* (ATP-PFK) (AF298119), *B. burgdorferi* (putative PFK) (F70190), *T. pallidum* (A71366), *Propionibacterium shermanii* (A41169), *Mycoplasma genitalium* (G64223), *Thermus thermophilus* (P21777), *T. maritima* (ATP-PFK) (C72406), *Aquifex aeolicus* (O67605), *E. coli* (KIECFA), *Lactococcus lactis* (JN0614), *Lactobacillus delbrueckii* (A48663), *Bacillus subtilis* (A69675), *Thermoproteus tenax* (CAA74985), *Dictyoglomus thermophilum* (AF268276.1), *S. coelicolor* A3(2) (PFK1) (OO8333), *A. methanolica* (PP_i-PFK) (Q59126), *S. coelicolor* A3(2) (putative PFK) PFK2 (AL138978.1), *S. coelicolor* A3(2) (putative PFK) PFK3 (AL391017.1), *M. tuberculosis* (O53257), *M. leprae* (O33106), *Saccharomyces cerevisae* alpha subunit (NP011756.1), *S. cerevisae* beta subunit (NP013932), rat (A53047), rabbit (P00125128), and human muscle (227448). Bootstrap values, based on 100 replicates, are indicated at the branch points. The asterisks indicate putative PFKs.

of RuMP cycle enzymes by glucose (13) (Table 2 and Fig. 2), will have strong negative effects on the RuMP cycle during growth on mixtures of glucose plus methanol in batch cultures. This explains previous observations that, during growth on such mixtures, methanol is used only as an additional energy source (oxidation to carbon dioxide) and not for carbon assimilation via the RuMP cycle (Fig. 1) (14). The data show that the ATP-PFK regulatory and kinetic properties of *A. methanolica* are finely tuned to its specific physiological role as a RuMP cycle enzyme.

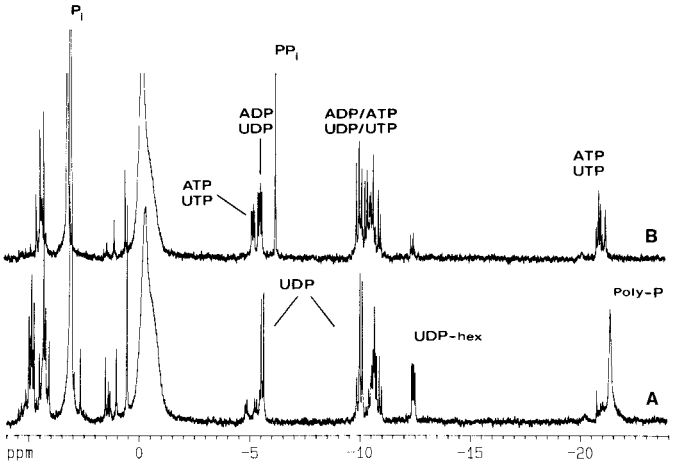

FIG. 6. ^{31}P-NMR spectra of perchloric acid extracts of *A. methanolica* cells grown on mineral medium containing 60 mM methanol (spectrum A) or 10 mM glucose (spectrum B). Resonance assignments are indicated above each peak: ADP, ATP, UDP, UTP, UDP-hex (uridine diphosphohexoses, such as UDP-*N*-acetylglucosamine), PP_i, P_i (inorganic phosphate), and poly-P (polyphosphate).

Little is known at the moment about (poly)phosphate metabolism in actinomycetes. Several interesting observations were made with *A. methanolica*. During growth on glucose, *A. methanolica* employs a PP_i-PFK (3) and a glucose kinase that uses not only ATP and GTP (3) as phosphogroup donors but also polyphosphates (P5–P75) (this study and data not shown). Similar glucose kinase activities have been studied previously in *Actinomyces naeslundii* (35) and *M. tuberculosis* (23). PP_i accumulation was readily detectable in glucose-grown cells, whereas no PP_i was found in methanol-grown cells (Fig. 6). Similar PP_i levels were also reported for other organisms possessing PP_i-linked enzyme activities, e.g., *Propionibacterium freudenreichii* (28, 29) and *A. naeslundii* (35). PP_i is produced in nucleic acid and protein biosynthesis and by metabolic cycling between glycogen and glucose-1-phosphate through the action of UDP-glucose synthase, glycogen synthase, and glycogen phosphorylase (12). Large differences in glycogen levels, however, were not observed between glucose- and methanol-grown cells of *A. methanolica* (data not shown). It is also possible that glucose uptake in *A. methanolica* is associated with PP_i release, but this remains to be studied experimentally. The source of PP_i during growth of *A. methanolica* thus has yet to be identified.

ACKNOWLEDGMENTS

A.M.C.R.A. was supported by JNICT (Portugal Grants BD808-IF-90; Praxis XXI-BD-2798-94).

We thank H. J. Hektor for assistance in the continuous culture experiments.

REFERENCES

1. **Alves, A. M. C. R.** 1997. Regulation of glucose metabolism in the actinomycetes *Amycolatopsis methanolica* and *Streptomyces coelicolor* A3(2). Ph.D. thesis. University of Groningen, Groningen, The Netherlands.
2. **Alves, A. M. C. R., G. J. W. Euverink, and L. Dijkhuizen.** 1997. Identification of ATP-dependent phosphofructokinase as a regulatory step in the glycolytic pathway of the actinomycete *Streptomyces coelicolor* A3(2). Appl. Environ. Microbiol. **63:**956–961.
3. **Alves, A. M. C. R., G. J. W. Euverink, H. J. Hektor, G. I. Hessels, J. van der Vlag, J. W. Vrijbloed, D. H. A. Hondmann, J. Visser, and L. Dijkhuizen.** 1994. Enzymes of glucose and methanol metabolism in the actinomycete *Amycolatopsis methanolica*. J. Bacteriol. **176:**6827–6835.
4. **Alves, A. M. C. R., W. G. Meijer, J. W. Vrijbloed, and L. Dijkhuizen.** 1996. Characterization and phylogeny of the *pfp* gene of *Amycolatopsis methanolica* encoding PP_i-dependent phosphofructokinase. J. Bacteriol. **178:**149–155.
5. **Balogh, A., J. H. Wong, C. Wotzel, J. Soll, C. Cseke, and B. B. Buchanan.** 1984. Metabolite-mediated catalyst conversion of PFK and PFP: a mechanism of enzyme regulation in green plants. FEBS Lett. **169:**287–292.
6. **Berger, S. A., and P. R. Evans.** 1990. Active-site mutants altering the cooperativity of *E. coli* phosphofructokinase. Nature **343:**575–576.
7. **Birnboim, H. C., and J. Doly.** 1979. A rapid alkaline extraction procedure for screening recombinant plasmid DNA. Nucleic Acids Res. **7:**1513–1523.
8. **Bradford, M. M.** 1976. A rapid and sensitive method for the quantitation of microgram quantities of protein utilizing the principle of protein-dye binding. Anal. Biochem. **72:**248–254.
9. **Buschmeir, B.** 1985. Purification and properties of 1-PFK from *Escherichia coli*. FEMS Microbiol. Lett. **29:**231–235.
10. **Dabbs, E. R., B. Gowan, S. Quan, and S. J. Andersen.** 1995. Development of improved *Rhodococcus* plasmid vectors and their use in cloning genes of potential commercial and medical importance. Biotechnologia **7–8:**129–135.
11. **Daldal, F., J. Babul, and D. G. Fraenkel.** 1982. An alteration in phosphofructokinase 2 of *Escherichia coli* which impairs gluconeogenic growth and improves growth on sugars. Eur. J. Biochem. **126:**373–379.
12. **Dawes, E. A., and P. E. Senior.** 1973. The role and regulation of energy reserve polymers in microorganisms. Adv. Microb. Physiol. **10:**135–166.
13. **de Boer, L., G. J. W. Euverink, J. van der Vlag, and L. Dijkhuizen.** 1990. Regulation of methanol metabolism in the facultative methylotroph *Nocardia* sp. 239 during growth on mixed substrates in batch- and continuous cultures. Arch. Microbiol. **153:**337–343.
14. **de Boer, L., M. van Rijssel, G. J. W. Euverink, and L. Dijkhuizen.** 1989. Purification, characterization and regulation of a monomeric L-phenylalanine dehydrogenase from the facultative methylotroph *Nocardia* sp. 239. Arch. Microbiol. **153:**12–18.
15. **Dijkhuizen, L., P. R. Levering, and G. E. de Vries.** 1992. The physiology and biochemistry of aerobic methanol-utilizing Gram-negative and Gram-positive bacteria, p. 149–181. *In* T. Atkinson and R. F. Sherwood (ed.), Methane and methanol utilizers. Plenum Press, New York, N.Y.
16. **Dijkhuizen, L., and I. G. Sokolov.** 1984. Regulation of oxidation and assimilation of one-carbon compounds in methylotrophic bacteria, p. 127–148. *In* I. Goldberg and J. S. Rokem (ed.), Biology of methylotrophs. Butterworths-Heinemann, London, United Kingdom.
17. **Doelle, H. W.** 1975. ATP-sensitive and ATP-insensitive phosphofructokinase in *Escherichia coli* K-12. Eur. J. Biochem. **50:**335–342.
18. **Fothergill-Gilmore, L. A., and P. A. M. Michels.** 1993. Evolution of glycolysis. Prog. Biophys. Mol. Biol. **59:**105–235.
19. **Fraenkel, D. G.** 1987. Glycolysis, pentose phosphate pathway, and Entner-Doudoroff pathway, p. 142–151. *In* F. C. Neidhardt, J. L. Ingraham, B. Magasanik, K. B. Low, and M. Schaechter (ed.), *Escherichia coli* and *Salmonella typhimurium*. Cellular and molecular biology. American Society for Microbiology, Washington, D.C.
20. **Hektor, H. J., and L. Dijkhuizen.** 1996. Mutational analysis of primary alcohol metabolism in the methylotrophic actinomycete *Amycolatopsis methanolica*. FEMS Microbiol. Lett. **144:**73–81.
21. **Hofmann, E.** 1976. The significance of phosphofructokinase to the regulation of carbohydrate metabolism. Rev. Physiol. Biochem. Pharmacol. **75:**1–67.

22. **Hondmann, D. H. A., and J. Visser.** 1990. Screening method for large numbers of dye-adsorbents for enzyme purification. J. Chromatogr. **510:**155–164.
23. **Hsieh, P. C., T. H. Kowalczyk, and N. F. B. Philips.** 1996. Kinetic mechanisms of polyphosphate glucokinase from *Mycobacterium tuberculosis*. Biochemistry **35:**9772–9781.
24. **Kengen, S. W. M., J. E. Tuininga, F. A. M. Debok, A. J. M. Stams, and W. M. de Vos.** 1995. Purification and characterization of a novel ADP-dependent glucokinase from the hyperthermophilic archaeon *Pyrococcus furiosus*. J. Biol. Chem. **270:**30453–30457.
25. **Kotzlar, D., and H. Buc.** 1977. Two *Escherichia coli* fructose-6-phosphate kinases. Preparative purification, oligomeric structure and immunological studies. Biochim. Biomed. Acta **484:**35–48.
26. **Kotzlar, D., and H. Buc.** 1981. Regulatory properties of phosphofructokinase 2 from *Escherichia coli*. Eur. J. Biochem. **117:**569–574.
27. **Laemmli, U. K., and K. Favre.** 1973. Maturation of the head of bacteriophage T4. J. Mol. Biol. **80:**575–599.
28. **Mertens, E.** 1991. Pyrophosphate-dependent phosphofructokinase, an anaerobic glycolytic enzyme? FEBS Lett. **285:**1–5.
29. **Mertens, E.** 1993. ATP versus pyrophosphate: glycolysis revisited in parasitic protists. Parasitol. Today **9:**122–126.
30. **Mertens, E., and M. Müller.** 1990. Glucokinase and fructokinase of *Trichomonas vaginalis* and *Tritrichomonas foetus*. J. Protozool. **37:**384–388.
31. **Reeves, R. E., D. J. South, H. J. Blytt, and L. G. Warren.** 1974. Pyrophosphate: D-fructose 6-phosphate 1-phosphotransferase. A new enzyme with the glycolytic function 6-phosphate 1-phosphotransferase. J. Biol. Chem. **249:**7737–7741.
32. **Sambrook, J., E. F. Fritsch, and T. Maniatis.** 1989. Molecular cloning: a laboratory manual, 2nd ed. Cold Spring Harbor Laboratory, Cold Spring Harbor, N.Y.
33. **Selig, M., K. B. Xavier, H. Santos, and P. Schönheit.** 1997. Comparative analysis of Embden-Meyerhof and Entner-Doudoroff glycolytic pathways in hyperthermophilic archaea and the bacterium *Thermotoga*. Arch. Microbiol. **167:**217–232.
34. **Shirakihara, Y., and P. R. Evans.** 1988. Crystal structure of the complex of phosphofructokinase from *Escherichia coli* with its reaction products. J. Mol. Biol. **204:**973–994.
35. **Takahashi, N., S. Kalfas, and T. Yamada.** 1995. Phosphorylating enzymes involved in glucose fermentation of *Actinomyces naeslundii*. J. Bacteriol. **177:**5806–5811.
36. **Thompson, J. D., D. G. Higgins, and T. J. Gibson.** 1994. CLUSTAL W: improving the sensitivity of progressive multiple sequence alignment through sequence weighting, position-gap penalties and weight matrix choice. Nucleic Acids Res. **22:**4673–4680.
37. **Uyeda, K.** 1979. Phosphofructokinase. Adv. Enzymol. **48:**193–244.
38. **van de Peer, Y., and R. de Wachter.** 1994. Construction of evolutionary distance trees with Treecon for Windows: accounting for variation in nucleotide substitution rate among sites. Comput. Appl. Biosci. **10:**569–570.
39. **Vishniac, W., and W. Santer.** 1957. The *thiobacilli*. Bacteriol. Rev. **21:**195–213.
40. **Vogt-Singer, M. E., and W. R. Finnerty.** 1988. Construction of an *Escherichia coli-Rhodococcus* shuttle vector and plasmid transformation in *Rhodococcus* spp. J. Bacteriol. **170:**638–645.
41. **Voss, H., C. Schwager, V. Wirkner, J. Zimmermann, H. Erfle, N. Hewitt, T. Rupp, J. Stegemann, and W. Ansorge.** 1992. New procedure for automated DNA sequencing with multiple internal labelling by fluorescent dUTP. Methods Mol. Cell. Biol **3:**30–34.
42. **Vrijbloed, J. W., J. Madon, and L. Dijkhuizen.** 1995. Transformation of the methylotrophic actinomycete *Amycolatopis methanolica* with plasmid DNA: stimulatory effect of a pMEA300-encoded gene. Plasmid **34:**96–104.
43. **Wray, W., T. Boulikas, V. P. Wray, and R. Hancock.** 1981. Silver staining of proteins in polyacrylamide gels. Anal. Biochem. **118:**197.
44. **Wright, F., and M. J. Bibb.** 1992. Codon usage in the G+C rich *Streptomyces* genome. Gene **113:**55–65.